

Low-Temperature Characteristics of a Silicon-Based Sub-THz Detector

A. R. Khisameeva^{a,*}, A. V. Shchepetilnikov^a, Ya. V. Fedotova^a, A. A. Dremin^a, and I. V. Kukushkin^a

^a Institute of Solid State Physics, Russian Academy of Sciences, Chernogolovka, Moscow oblast, 142432 Russia

*e-mail: akhisameeva@issp.ac.ru

Received September 17, 2022; revised October 5, 2022; accepted October 26, 2022

Abstract—Characteristics of a silicon-based sub-THz plasmonic detector are studied in a wide range of temperatures down to that of liquid nitrogen. The temperature dependences of the detector's sensitivity are obtained and its noise characteristics are studied. The frequency dependence of the sensitivity in the range of 70–120 GHz is measured at room temperature, and its maximum of 25 V/W is reached at 96 GHz. The noise equivalent power of the studied detector is estimated by assuming that Nyquist noise is the main source of noise, and the values of this power vary from 2×10^{-10} W Hz^{-1/2} at room temperature to 2×10^{-11} W Hz^{-1/2} at the temperature of liquid nitrogen. The current–voltage characteristics of the sub-THz detector are studied as well. It is found there is a singularity in the differential resistance and sensitivity that depends on the DC voltage applied during the transition from room to nitrogen temperature.

DOI: 10.3103/S1062873822700824

INTRODUCTION

Persistent study of the subterahertz range of frequencies has resulted in a new branch of modern physics and technology, the development of which is of fundamental importance to the physics of condensed matter [1], bio- [2] and astrophysics [3], and practical applications. Subterahertz technologies are increasingly used in telecommunications [4–7], medicine [2], security screening [8–10], and the nondestructive testing of quality of products [11].

A number of unique characteristics of electromagnetic radiation in the terahertz range of frequencies creates a wide variety of scientific and technical problems that can be solved using terahertz technologies. Most materials (e.g., plastics, wood, rubber, and different composite materials) are transparent in the subterahertz range of the spectrum. The relatively short wavelength of such radiation provides reasonable spatial resolution when visualizing objects, a low energy of photons, and thus non-ionizing radiation that is safe for humans and animals.

The development of sensitive elements for radiation in the terahertz range of frequencies is the key to progress in the field of terahertz technologies. Modern THz and sub-THz detectors can be used as high electron mobility transistors [12], field transistors [13], Schottky diodes [14], microbolometers [15], pyroelectric sensors [16], and Golay cells [17]. From the viewpoint of the temporal response, manufacturing cost, and compatibility with current technological and processing chains, one of the most promising ways of

detecting THz radiation is converting incident radiation into an alternating potential of a relativistic plasma wave using a broadband antenna array deposited on a crystal surface. The physical characteristics of this plasma excitation in a hybrid GaAs/AlGaAs two-dimensional electron system based on quantum wells were studied in [18, 19]. Due to the asymmetry of a plasmonic waveguide, the oscillating potential of a plasma wave is rectified to yield a reliably measurable photoresponse [20]. As was shown in [21], this plasmonic THz detector has an extremely fast temporal response of less than 150 ps.

Continuing studies on detectors of sub-THz radiation based on GaAs/AlGaAs heterostructures [20–22], in this work we study the characteristics of such a silicon-based detector in a relatively wide sub-THz range of frequencies at different temperatures. It should be emphasized that a Si-based detector has considerable advantages that include simple integration of microcircuits and compatibility with modern processing chains, resulting in low costs. Studies of the temperature dependences of sensitivity S and noise equivalent power NEP are also of particular interest. For a number of scientific and practical problems in, e.g., astrophysics [2] and condensed matter physics [1], we can use cooled detectors so long as their noise characteristics are enhanced. Cooling systems are also becoming smaller and easier to obtain, and often do not require expensive cryogenic fluids or the related complex infrastructure.

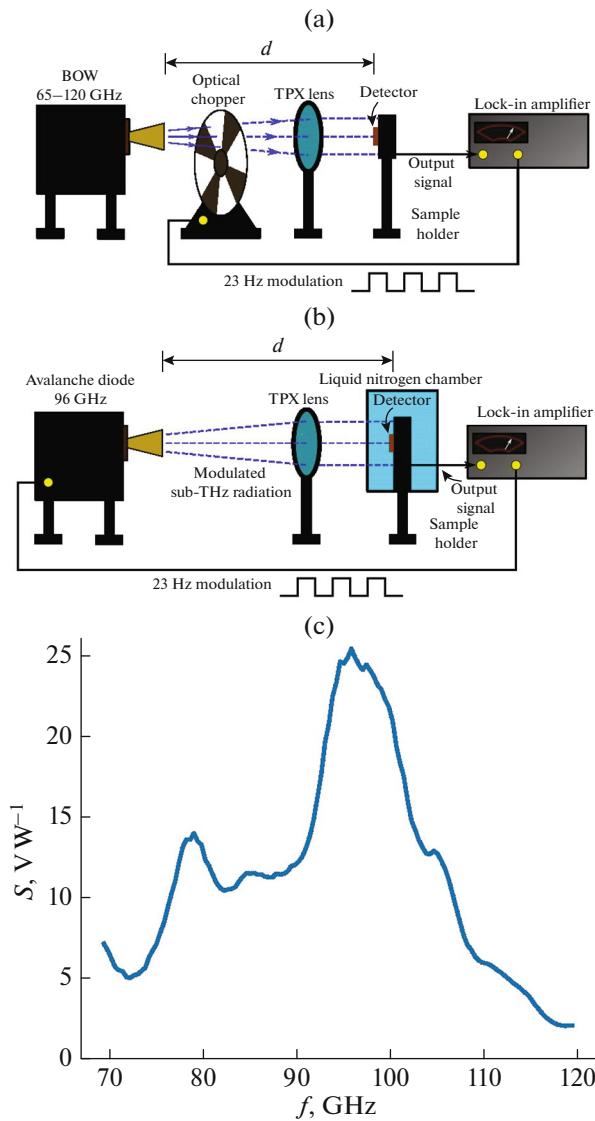


Fig. 1. (a) Experimental setup for measuring the frequency response of the detector. (b) Experimental setup for measuring the low-temperature characteristics of the detector, and (c) frequency response of sensitivity S of the silicon-based detector of sub-THz radiation.

In this work, we studied the characteristics of plasmonic sub-THz detectors at low temperatures (up to the temperature of liquid nitrogen $T = 77$ K). Such detectors can be integrated into large arrays to form THz radiation chambers [10, 23], allowing us to increase their sensitivity without making a device too bulky or expensive.

EXPERIMENTAL

Our sample was a plasmonic detector of sub-THz radiation, the design and main principle of operation

of which were described in [20–22]. The characteristic size of the detector was 3×3 mm².

The frequency characteristics of the detector were measured at room temperature using the quasi-optical scheme shown in Fig. 1a. The sources of sub-THz radiation were a backward wave oscillator (BWO) operating in the 65–120 GHz range of frequencies (the output power was no more than 100 mW and could be reduced using a quasi-optical attenuator) and a generator based on an avalanche diode (AD) with fixed frequency $f = 96$ GHz and an output power of 1 W, which could be reduced from 0 to -40 dB using a built-in waveguide attenuator. The power level of radiation incident on the sample was monitored using an independently calibrated pyroelectric detector. Measurements were made in a linear-power mode.

A TPX quasi-optical lens with a focal length of 60 mm and a diameter of 120 mm was installed in the optical path to compensate for the divergence of the initial beam at the output of sub-THz radiation sources. The distance between the output of the horn antenna and the lens was equal to the focal length. The silicon detector was placed on a special holder in the center of the obtained parallel beam with an area much larger than the size of the detector. The distance between the detector and the source of THz radiation was $d = 30$ cm. The output radiation was modulated with an optical modulator at a frequency $f_{\text{mod}} = 23$ Hz. The photovoltage on the silicon detector was measured using a lock-in amplifier tuned to the amplitude modulation frequency of radiation.

The silicon detector was placed into a special chamber with a window transparent to sub-THz radiation in order to measure temperature. The detector was mounted on a massive cold stand cooled with liquid nitrogen. The time needed for the detector to cool to nitrogen temperature was typically several hours. A special calibrated thermometer was mounted close to the detector. The scheme for measuring low-temperature characteristics of the detector is shown in Fig. 1b.

RESULTS AND DISCUSSION

The dependence of sensitivity S of the silicon detector on frequency $f = 70$ –120 GHz of incident sub-THz radiation is shown in Fig. 1c. The measurements were made at room temperature, and the characteristic resistance of the detector at low direct currents was $R = 2.2$ k Ω . This dependence shows that the maximum of sensitivity S of the sub-THz detector was in the range $f = 96$ –100 GHz and reached maximum value $S = 25$ V W⁻¹. Note that the frequency of the avalanche diode used to study the low-temperature characteristics of the detector was in the abovementioned range of frequencies. The observed pattern of the frequency dependence was due to interference

from electromagnetic waves inside the silicon substrate and was studied in [22].

Figure 2 shows results from temperature measurements of the main characteristics of the sub-THz silicon detector. Structural resistance R was measured using a lock-in detector while alternating current $I = 1 \mu\text{A}$ flowed through the sample. Lowering the temperature from room to that of liquid nitrogen (Fig. 2a) changed resistance R from 2.2 to 6.9 $\text{k}\Omega$. Such a negligible change in resistance indicates the structure's contacts work up to liquid nitrogen temperature, and the detector retained its operational ability throughout the specified range of temperatures.

The next step was to measure the change in sensitivity S as the temperature fell. Our results showed a much stronger change in sensitivity. The value of S rose by more than an order of magnitude, from 25 to 300 V W^{-1} . Lowering the detector's temperature to that of liquid nitrogen thus improved the detector's sensitivity considerably. The pattern of dependence (a sharp increase in sensitivity at low temperatures) indicates a further reduction in temperature would also improve the characteristics of the plasmonic detector.

Note that both the resistance of the detector and its sensitivity rose as the temperature fell. It is therefore correct to use noise characteristics for a reliable estimate of the improvement in the detecting characteristics of a sensitive element. Let us estimate the noise equivalent power (NEP) of the detector by assuming the main contribution to noise v_n at the detector's output was of a Nyquist nature:

$$v_n = \sqrt{4kTR}, \quad (1)$$

where k is the Boltzmann constant, and T and R are the temperature and resistance of the detector. The noise equivalent power can then be calculated as

$$\text{NEP} = \sqrt{4kTR}/S. \quad (2)$$

Figure 2c shows the temperature dependence obtained for the NEP of the silicon detector. It changed from 2×10^{-10} to $2 \times 10^{-11} \text{ W Hz}^{-1/2}$ upon lowering the temperature to that of liquid nitrogen. We may therefore conclude that the noise characteristics of the detector were improved by an order of magnitude as the temperature fell.

We also studied the possibility of improving the characteristics of the detector by applying a constant voltage to its output. The direct current flowing through the detector and the alternating photovoltage at its output were measured. The power of the incident radiation was unchanged. These measurements were made at both $T = 300 \text{ K}$ and liquid nitrogen temperature. Results are presented in Fig. 3. The plots in Figs. 3a and 3b show the dependence of the differential resistance on the current flowing through the sam-

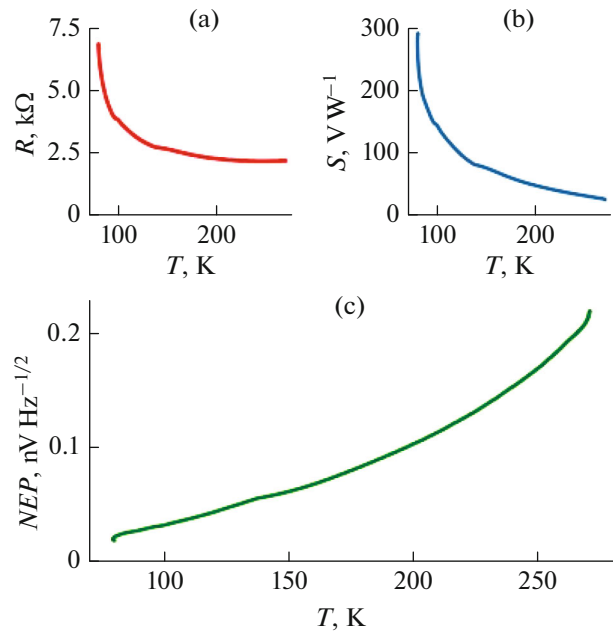


Fig. 2. Measured temperature dependences of (a) resistance R , (b) sensitivity S of the detector, and (c) power noise equivalent NEP obtained by assuming the main contribution to photovoltage fluctuations came from the thermal Nyquist noise.

ple. This dependence was monotonic at room temperature. In contrast, a pronounced maximum in the differential resistance appeared at a low temperatures. The detector thus became much more nonlinear as the temperature fell, which (among other things) also improved its sensitivity.

Figures 3c and 3d show the dependences of the detector's sensitivity to DC voltage applied at room and liquid nitrogen temperatures, respectively. While the application of direct current at room temperature resulted in a negligible improvement in the sensitivity of the detector, the value of S was already maximal in the vicinity of zero applied voltage at $T = 77 \text{ K}$.

CONCLUSIONS

This work was a continuation of earlier studies of the characteristics of a GaAs-based plasmonic THz detector. We studied the low-temperature characteristics of a silicon-based detector of sub-THz radiation in a wide range of temperatures. When the temperature was lowered to that of liquid nitrogen, the resistance of the detector rose from 2.2 to 6.6 $\text{k}\Omega$, while its sensitivity grew by around 10 times. The noise characteristics also grew by an order of magnitude as the temperature fell. The dependences of the differential resistance and sensitivity of the detector on the applied DC voltage were also studied. At the temperature of liquid nitro-

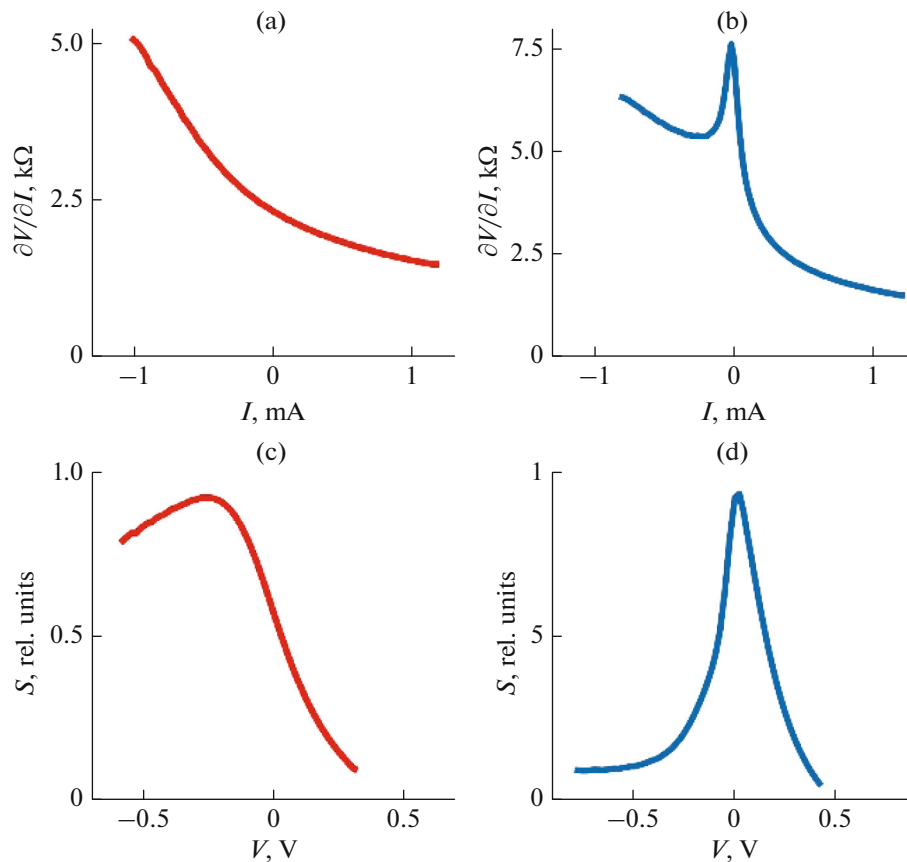


Fig. 3. Differential resistance of the detector for various bias currents I at (a) room and (b) liquid nitrogen temperatures; detector sensitivity S for various bias voltages V at (c) room and (d) liquid-nitrogen temperatures.

gen and zero external voltage, there was a singularity in the differential resistance and sensitivity.

OPEN ACCESS

This article is licensed under a Creative Commons Attribution 4.0 International License, which permits use, sharing, adaptation, distribution and reproduction in any medium or format, as long as you give appropriate credit to the original author(s) and the source, provide a link to the Creative Commons license, and indicate if changes were made. The images or other third party material in this article are included in the article's Creative Commons license, unless indicated otherwise in a credit line to the material. If material is not included in the article's Creative Commons license and your intended use is not permitted by statutory regulation or exceeds the permitted use, you will need to obtain permission directly from the copyright holder. To view a copy of this license, visit <http://creativecommons.org/licenses/by/4.0/>.

FUNDING

This work was supported by the Russian Science Foundation, project no. 19-72-30003.

CONFLICT OF INTEREST

The authors declare they have no conflicts of interest.

REFERENCES

1. Shuvaev, A., Muravev, V.M., Gusikhin, P.A., et al., *Phys. Rev. Lett.*, 2021, vol. 126, no. 13, p. 136801.
2. Siegel, P.H., *IEEE Trans. Microwave Theory Tech.*, 2004, vol. 52, no. 10, p. 2438.
3. Siegel, P.H., *IEEE Trans. Antennas Propag.*, 2007, vol. 55, no. 11, p. 2957.
4. Federici, J. and Moeller, L., *J. Appl. Phys.*, 2010, vol. 107, no. 11, p. 111101.
5. Song, H.J. and Nagatsuma, T., *IEEE Trans. Terahertz Sci. Technol.*, 2011, vol. 1, no. 1, p. 256.
6. Koenig, S., Lopez-Diaz, D., Antes, J., et al., *Nat. Photonics*, 2013, vol. 7, no. 12, p. 977.
7. Chen, Z., Ma, X., Zhang, B., et al., *China Commun.*, 2019, vol. 16, no. 2, p. 1.
8. Ogawa, Y., Kawase, K., Yamashita, M., et al., *Proc. CLEO Conf.*, San Francisco, 2004, p. 3.
9. Shen, Y.C., Lo, A.T., Taday, P.F., et al., *Appl. Phys. Lett.*, 2005, vol. 86, no. 24, p. 241116.

10. Tzydynzhapov, G., Gusikhin, P., Muravev, V., et al., *J. Infrared, Millimeter, Terahertz Waves*, 2020, vol. 41, no. 6, p. 632.
11. Shchepetilnikov, A.V., Gusikhin, P.A., Muravev, V.M., et al., *Appl. Opt.*, 2021, vol. 60, no. 33, p. 10448.
12. Dyakonov, M.I. and Shur, M.S., *IEEE Trans. Electron Devices*, 1996, vol. 43, no. 10, p. 1640.
13. Lü, J.Q. and Shur, M.S., *Appl. Phys. Lett.*, 2001, vol. 78, no. 17, p. 2587.
14. Fetterman, H.R., Clifton, B.J., Tannenwald, P.E., et al., *Appl. Phys. Lett.*, 1974, vol. 24, no. 2, p. 70.
15. Karasik, B.S., Sergeev, A.V., and Prober, D.E., *IEEE Trans. Terahertz Sci. Technol.*, 2011, vol. 1, no. 1, p. 97.
16. Whatmore, R.W., *Rep. Prog. Phys.*, 1986, vol. 49, no. 12, p. 1335.
17. Fernandes, L.O.T., Kaufmann, P., Marcon, R., et al., *Proc. XXXth URSI General Assembly and Scientific Symposium*, Istanbul, 2011, p. 1.
18. Muravev, V.M., Gusikhin, P.A., Andreev, I.V., et al., *Phys. Rev. Lett.*, 2015, vol. 114, no. 10, p. 106805.
19. Muravev, V.M., Gusikhin, P.A., Zarezin, A.M., et al., *Phys. Rev. B*, 2019, vol. 99, no. 24, p. 241406.
20. Muravev, V.M. and Kukushkin, I.V., *Appl. Phys. Lett.*, 2012, vol. 100, no. 8, p. 082102.
21. Murav'ev, V.M., Solov'ev, V.V., Fortunatov, A.A., et al., *JETP Lett.*, 2016, vol. 103, no. 12, p. 792.
22. Shchepetilnikov, A.V., Kaysin, B.D., Gusikhin, P.A., et al., *Opt. Quantum Electron.*, 2019, vol. 51, no. 12, p. 376.
23. Shchepetilnikov, A.V., Gusikhin, P.A., Muravev, V.M., et al., *J. Infrared, Millimeter, Terahertz Waves*, 2020, vol. 41, no. 6, p. 655.

Translated by N. Podymova